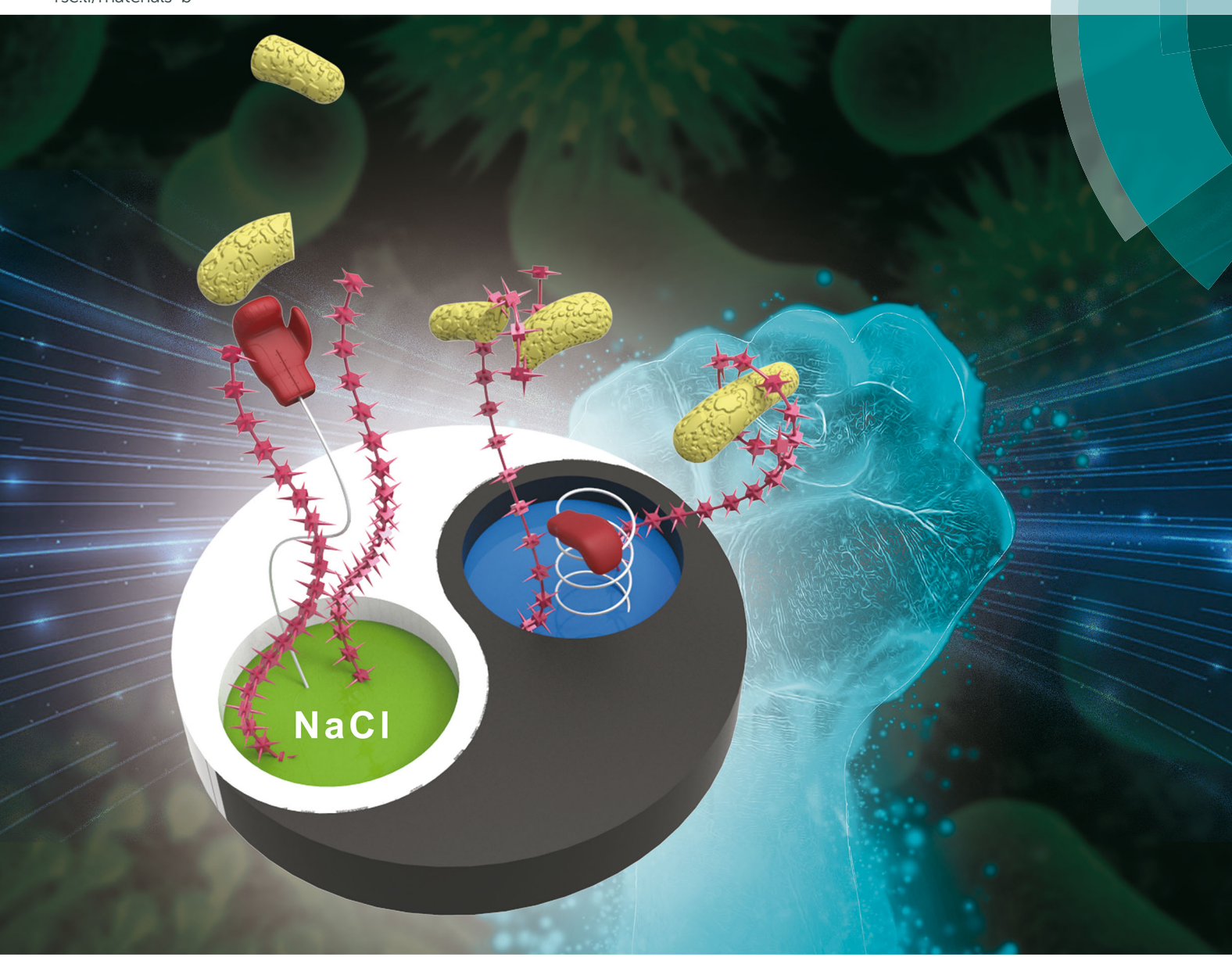
Journal of Materials Chemistry B

Materials for biology and medicine rsc.li/materials-b



ISSN 2050-750X



PAPER

Jintao Yang, Jie Zheng *et al*.

Design of salt-responsive and regenerative antibacterial polymer brushes with integrated bacterial resistance, killing, and release properties

Journal of Materials Chemistry B



PAPER



Cite this: *J. Mater. Chem. B*, 2019, 7, 5762

Design of salt-responsive and regenerative antibacterial polymer brushes with integrated bacterial resistance, killing, and release properties†

Yang Wang,^a Jiahui Wu,^a Dong Zhang,^b Feng Chen,^a Ping Fan,^a Mingqiang Zhong,^a Shengwei Xiao,^c Yung Chang, ^b Xiong Gong, ^e Jintao Yang*^a and Jie Zheng ^b*^b

The development of smart materials and surfaces with multiple antibacterial actions is of great importance for both fundamental research and practical applications, but this has proved to be extremely challenging. In this work, we proposed to integrate salt-responsive polyDVBAPS (poly(3-(dimethyl(4-vinylbenzyl) ammonio)propyl sulfonate)), antifouling polyHEAA (poly(N-hydroxyethyl acrylamide)), and bactericidal TCS (triclosan) into single surfaces by polymerizing and grafting polyDVBAPS and polyHEAA onto the substrate in a different way to form two types of polyDVBAPS/poly(HEAA-q-TCS) and poly(DVBAPS-b-HEAA-q-TCS) brushes with different hierarchical structures, as confirmed by X-ray photoelectron spectroscopy (XPS), atom force microscopy (AFM), and ellipsometry. Both types of polymer brushes demonstrated their tri-functional antibacterial activity to resist bacterial attachment by polyHEAA, to release $\sim 90\%$ of dead bacteria from the surface by polyDVBAPS, and to kill \sim 90% of bacteria on the surface by TCS. Comparative studies also showed that removal of any component from polyDVBAPS/poly(HEAA-q-TCS) and poly(DVBAPS-b-HEAA-q-TCS) compromised the overall antibacterial performance, further supporting a synergistic effect of the three compatible components. More importantly, the presence of salt-responsive polyDVBAPS allowed both brushes to regenerate with almost unaffected antibacterial capacity for reuse in multiple kill-and-release cycles. The tri-functional antibacterial surfaces present a promising design strategy for further developing next-generation antibacterial materials and coatings for antibacterial applications.

Received 28th June 2019, Accepted 7th August 2019

DOI: 10.1039/c9tb01313j

rsc.li/materials-b

Introduction

Bacteria in nature have a long-term symbiotic relationship with humans, and most of them are responsible for many lethal and infectious diseases, ^{1–4} including diarrhea caused by *Escherichia coli*, osteomyelitis caused by *Staphylococcus aureus*, and tuberculosis

caused by Mycobacterium tuberculosis. 5,6 More importantly, almost all bacteria have developed a time-dependent resistance ability against any antibiotics due to natural evolution.⁷ Continuously growing bacterial resistance with a diminishing antibiotic pipeline poses serious problems for many biomedical and industrial applications.8 Among different antibacterial applications, it is estimated that ~80% of human infections occurs on bacteriacontaminated surfaces, which usually involves initial bacterial attachment, subsequent colonization, and final biofilm formation. Once the biofilm is formed, it is too late or too difficult to remove live/dead bacteria from the surfaces, which in turn enhances bacterial antibiotic resistance and bacterial infections. 9-13 Thus, the development of broad-spectrum antibacterial materials and smart surfaces/coatings to prevent early bacterial attachment and colonization is considered as an effective strategy for a variety of practical applications. 14-17

Many different antibacterial surfaces with antifouling, ^{18–20} bactericidal, ^{21,22} and/or bacterial release ^{23,24} have been developed for resisting bacterial adhesion. ^{25–29} These antibacterial surfaces generally involve three main mechanisms to achieve their

^a College of Materials Science & Engineering Zhejiang, University of Technology, Hangzhou 310014, China. E-mail: yangjt@zjut.edu.cn

b Department of Chemical and Biomolecular Engineering, The University of Akron, Akron, Ohio 44325, USA. E-mail: zhengj@uakron.edu

^c School of Pharmaceutical and Chemical Engineering, Taizhou University, Jiaojiang 318000, China

^d Department of Chemical Engineering R&D Center for Membrane Technology, Chung Yuan Christian University, Chungli, Taiwan

^e Department of Polymer Engineering, The University of Akron, Akron, Ohio 44325, USA

 $[\]dagger$ Electronic supplementary information (ESI) available: Figures showing anti-bacterial performance of polyDVBAPS/polyHEAA-based brushes against S. aureus, and antibacterial performance of polyHEAA, polyDVBAPS_/polyHEAA and poly(DVBAPS-b-HEAA) brushes in multiple antifouling, killing and release cycles. See DOI: 10.1039/c9tb01313j

antibacterial activity: (i) using antifouling materials (e.g., hydrophilic and zwitterionic polymers) to prevent the initial bacterial attachment; (ii) using synthetic or natural biocides to kill the attached bacteria; and (iii) using stimuli-responsive materials to release the dead bacteria. Thus, a general design strategy for an effective antibacterial surface is to integrate at least two antibacterial mechanisms into a coating surface, which has shown better antibacterial activity than a surface with a single antibacterial mechanism. For instance, some surfaces that integrate both antifouling and bactericidal properties are able to resist bacterial attachment/growth and kill bacteria on the surface simultaneously, demonstrating the "antifouling and killing" mechanism. However, the attached dead bacteria still contaminate the surfaces and form a conditioning layer for subsequent bacterial attachment and biofilm development. To overcome this limit, another type of antibacterial surface was developed to combine both bacterial killing and release functions (i.e. "killing and release" strategy) for achieving surface regeneration and maintaining antibacterial efficiency after dead bacteria are completely or largely released.^{30–35} However, a challenge still remains. Most of the killing-andrelease antibacterial surfaces usually have relatively limited surface regeneration capability and also require a longer time (e.g., hours to days) and more complicated stimuli to realize surface regeneration due to the lack of antifouling property. In most cases, after several cycles of surface regeneration, the surfaces will lose their antibacterial activity to a larger extent.

Despite their general effectiveness, dual-functional antibacterial surfaces with either "killing-and-antifouling" or "killing-andrelease" mechanisms have inherent limits and are still not sufficient to achieve the best antibacterial efficacy for practical applications. Thus, it is highly desirable to design an ideal antibacterial surface that integrates three complement properties of antifouling background coating, bacterial killing, and bacterial release into one surface, in which an antifouling coating prevents bacterial attachment, the bactericidal component actively kills the attached bacteria, and stimuli-responsive materials release dead bacteria and debris from the surface. Such tri-functional antibacterial surfaces are expected to be more effective for bacterial resistance, antimicrobial action, and fouling release in a reversible and controllable way for effective surface regeneration,³⁶ which will greatly expand antibacterial applications for biomedical materials and devices. To achieve this, here, we developed tri-functional, reusable antibacterial surfaces with integrated bacterial resistance, killing, and release properties. This antibacterial surface consisted of (1) a salt-responsive polymer of poly(3-(dimethyl(4-vinylbenzyl)ammonio)propyl sulfonate) (polyDVBAPS) for releasing the attached bacteria in response to salt solution, ²⁷ (2) a hydrophilic polymer of poly(*N*-hydroxyethyl acrylamide) (polyHEAA) as a super-low fouling background for preventing long-term bacterial colonization, and (3) a bactericidal agent of triclosan (TCS) for actively killing attached bacteria. To better understand the component-structure-property relationship of such antibacterial surfaces, we fabricated two different types of polymer brushes with hierarchical structures by (i) mixing poly-DVBAPS and polyHEAA to form mixed polyDVBAPS/polyHEAA

brushes and (ii) copolymerizing polyDVBAPS and polyHEAA to form poly(DVBAPS-b-HEAA)-block copolymer brushes, respectively. Furthermore, TCS was grafted onto polyHEAA of both poly-DVBAPS/polyHEAA and poly(DVBAPS-b-HEAA) brushes to impart bactericidal activity. The resultant antibacterial brushes were characterized for their surface composition, surface morphology, and chain conformation using X-ray photoelectron spectroscopy (XPS), atom force microscopy (AFM), and ellipsometry, followed by antibacterial tests using Escherichia coli (E. coli, Gram-negative) and Staphylococcus aureus (S. aureus, Gram-positive) in multiple kill-and-release cycles. Both brushes demonstrate not only their long-term surface resistance to bacteria, high bactericidal activity, and efficient bacterial release capability, but also robust surface regeneration ability for multiple bacterial killing-and-release cycles. Our design strategy and polymer systems offer a promising way to fabricate multifunctional and regenerable antibacterial surfaces for different antibacterial applications.

Materials and methods

Materials

Dimethylamine solution (40 wt% in H₂O), 1,3-propanesultone (98%), and 2,2,2-trifluoroethanol were purchased from Aladdin (Shanghai). N-(2-Hydroxyethyl) acrylamide (HEAA, stabilized with MEHO, 98%) was purchased from Sigma-Aldrich (Shanghai). Tris[2-(dimethylamino)-ethyl]amine (Me6TREN, 99%) was purchased from Tokyo Chemical Inc (TCI). Sodium N,N-diethyldithiocarbamate and [p-(chloromethyl)phenyl]trimethoxysilane were purchased from J&K (Beijing). The ATRP initiator that can be covalently grafted on silica wafer, 3-(2-bromoisobutyramido)propyl(trimethoxy)silane, was purchased from Gelest, Inc. (Morrisville, PA). 4-Vinlybenzyl chloride (90%) and oxalyl chloride (98%) were supplied by Energy Chemical (Shanghai). Triclosan (TCS, 97%) and dichloromethane (DCM, stabilized with amylene, 99.9%) were obtained from Shanghai Macklin Chemistry Co., Ltd. All the reagents mentioned above were used as received. Copper(1) bromide (CuBr, Shanghai Macklin Chemistry Co., Ltd) was purified by stirring in acetic acid, washing with ethanol, and then drying under vacuum. Methanol, toluene, acetonitrile, triethylamine (TEA) and all other solvents were obtained from Linfeng Chemical Reagent Co., Ltd (Shanghai) and purified according to standard methods. Water used in these experiments was purified using a Millipore water purification system with a maximum resistivity of 18.0 M Ω cm. The photoinitiator (4-trimethoxysilylphenyl) methyl N,N-diethylcarbamodithioate (SBDC) and the DVBAPS monomer were synthesized and purified using a previously published method. 37,38

Immobilization of initiators on silicon wafers

Silicon wafers (20 mm \times 15 mm) were ultrasonically cleaned in ethanol and deionized water, then immersed into a freshly prepared "piranha solution" (H_2O_2 /concentrated H_2SO_4 , 40:120, v/v) at 120 $^{\circ}C$ for \sim 0.5 h, rinsed with a copious amount of distilled water, and dried by nitrogen flow. Afterwards, the substrates were treated with plasma (CORONA Lab. CTP-2000, Nanjing, China)

for 1.5 min. Then, the cleaned wafers were placed into a dehydrated toluene solution containing either dual initiators (1.0 mmol of the ATRP initiator and 1.0 mmol of the PIMP initiator) for the preparation of the mixed brushes or a single initiator (2.0 mmol of the ATRP initiator) for the preparation of double-layer brushes overnight at room temperature, followed by repeated toluene, ethanol and deionized water rinsing to remove physically absorbed initiator molecules and then dried with nitrogen flow to obtain two types of initiator-modified surfaces.

Synthesis of mixed and double-layer polymer brushes

To fabricate the mixed polymer brushes, polyDVBAPS brushes were first prepared using the SI-ATRP method. Specifically, DVBAPS (0.56 g, 1.96 mmol) and Me6TREN (34.2 μL, 0.13 mmol) were dissolved in a mixture solution of 2,2,2-trifluoroethanol and deionized water (4.0 mL, v:v = 1:1), and degassed by nitrogen flow. The mixture solution was syringed into the sealed reaction tube containing CuBr (14.5 mg, 0.10 mmol) and the initiator-immobilized silicon wafers under nitrogen protection. Then, the reaction was conducted at different times of 4 h and 9 h to fabricate polyDVBAPS brushes with ~ 15 nm and ~30 nm thickness at room temperature, respectively, after which the wafers were collected, and repeatedly washed ultrasonically with saturated NaCl solution and deionized water to get polyDVBAPS brushes. Subsequently, the wafers with polyDVBAPS brushes fabricated above were placed into a quartz tube with the solution of HEAA (0.6 g, 5.21 mmol), methanol and deionized water (4.0 mL, v:v = 1:1), and a surface photoinitiated polymerization (SI-PIMP) of 40 min was conducted using a photo-reactor system (400 W high-pressure mercury lamp, ~380 nm) to fabricate the polyHEAA brush. The substrates were collected, washed with methanol and deionized water repeatedly to remove the absorbed free polymer, and dried with N2 flow at room temperature to get the wafers modified with mixed polyDVBAPS/polyHEAA brushes.

To fabricate the double-layer polymer brushes, the bottom polyDVBAPS layer with a thickness of $\sim\!35$ nm was first fabricated by SI-ATRP. A second layer of polyHEAA was then fabricated using another SI-ATRP. Briefly, HEAA (0.6 g, 5.21 mmol) and Me6TREN (34.2 μL , 0.13 mmol) were dissolved in a mixture solution of methanol and deionized water (4.0 mL, v:v=1:1), and degassed by nitrogen flow. The mixture solution was syringed into a sealed reaction tube containing CuBr (14.5 mg, 0.10 mmol) and polyDVBAPS-grafted wafer under nitrogen protection. Then, the reaction was conducted at room temperature for 24 h, after which the substrates were collected, repeatedly washed with methanol and deionized water, and dried with N2 flow at room temperature to get poly(DVBAPS-b-HEAA) brushes.

Immobilization of TCS onto mixed and double-layer polymer brushes

The immobilization of TCS on the polyHEAA brush was achieved following the previously published literature.³⁹ Briefly, TCS (4.35 g, 15 mmol) was dissolved in a mixture solution containing dry dichloromethane (15 mL) and TEA (3.14 mL, 7.5 mmol), and the

mixture was added dropwise into an anhydrous dichloromethane (7.5 mL) solution containing oxalyl chloride (1.92 mL, 22.5 mmol) and stirred under the protection of N_2 in an ice-bath for 2 h. Then, the reaction was maintained at room temperature for another 2 h. Subsequently, the solvent and the unreacted oxalyl chloride were removed by vacuum rotary evaporation to obtain the product. The as prepared HEAA-modified brushes were added to the solution of the product in anhydrous dichloromethane and stirred under the protection of N_2 at room temperature overnight. After the reaction, the TCS-grafted brushes were taken out from solution, ultrasonically cleaned with dichloromethane, ethanol, and deionized water successively, and dried with N_2 flow for further characterization.

Thickness of polymer brushes by ellipsometry

The thicknesses of polyHEAA, polyDVBAPS₁/polyHEAA, polyDVBAPS₂/polyHEAA and poly(DVBAPS-*b*-HEAA) brushes were measured *via* ellipsometry performed on an α -SE ellipsometer (J. A. Woollam Co., Lincoln, NE) with a He–Ne laser (λ = 632.8 nm) and an incident angle (70°).

Surface composition obtained via XPS

The surface composition of the samples was determined via X-ray photoelectron spectroscopy (XPS; PHI5000C ESCA) using a Mg K α anode mono-X-ray source at a power of 250 W (140 kV) under a vacuum of 1.0×10^{-8} Torr with a takeoff angle of 45° . The spectra were scanned over a range of 0–1000 eV, and the atomic concentrations of the elements were calculated by using the peak-area ratios.

Surface morphology and roughness obtained via AFM

Atomic force microscopy AFM (Bruker Daltonics Inc., USA) measurements were used to investigate the surface morphology of the polymer brushes in tapping mode. All images were acquired at a typical scan rate of 0.6 Hz with a scan range of 4.0 μ m. The root-mean-square (RMS) roughness was determined using the NanoScope Analysis software.

Contact angle measurement

The static contact angles (CAs) of the brushes were determined by Drop shape analysis (Eastern-Dataphy Instruments Co., Ltd, Beijing) using a sessile dropping method at ambient temperature. A 2 μL droplet of water and saturated NaCl solution was dropped on the surfaces for WCA recording. Four independent positions were determined on each sample to get averaged CA data.

Antibacterial assay

E. coli (Gram-negative) and *S. aureus* (Gram-positive) were used to test the antifouling, bactericidal and regeneration properties of the surfaces. The two types of bacteria were first incubated on Luria–Bertani (LB) agar medium at 37 °C overnight, then the bacterial colonies on the plates were inoculated into 40 mL of LB medium and shaken at 37 °C for 10 h. The bacterial solutions were then diluted with pure LB to OD values of 0.1 for *E. coli* and 0.05 for *S. aureus*, respectively. For antibacterial assay, the wafers were sterilized by 75% ethanol solution and rinsed with PBS before being placed into a 12-well sterile plate.

Subsequently, 3 mL of bacterial suspension solution was added into the well and cultured at 37 °C for a prespecified time (24 h for E. coli and 12 h for S. aureus, respectively) under 100 rpm shaking. After culturing, the samples were divided into two parts. The samples for testing the release property were placed into 1 M NaCl solution and gently shaken for 10 min, after which all the samples were washed with sterile PBS 3 times and stained by using the LIVE/DEAD BacLight Viability Kit (Thermo Fisher Scientific Inc., NY) for 15 min in the dark, rinsed with sterile PBS, and then observed using an Axio Observer A1 fluorescence microscope (Carl Zeiss Inc., Germany).

To examine long-term nonfouling, bactericidal and regeneration reliability of the surfaces, repeated "antifouling-killing-release" processes were conducted. The culture time of E. coli (OD value: 0.1) and S. aureus (OD value: 0.05) was 120 h and 72 h for one cycle, respectively. After that, the samples were regenerated and stained followed by the procedure above. For each antibacterial assay, at least three pieces of wafer were used and four different sites were used for fluorescent images for each sample. Therefore, at least twelve images were used for bacterial density analysis. Herein, three cycles were carried out, and both killing effectiveness and release ratio were calculated to evaluate the antimicrobial property of each cycle.

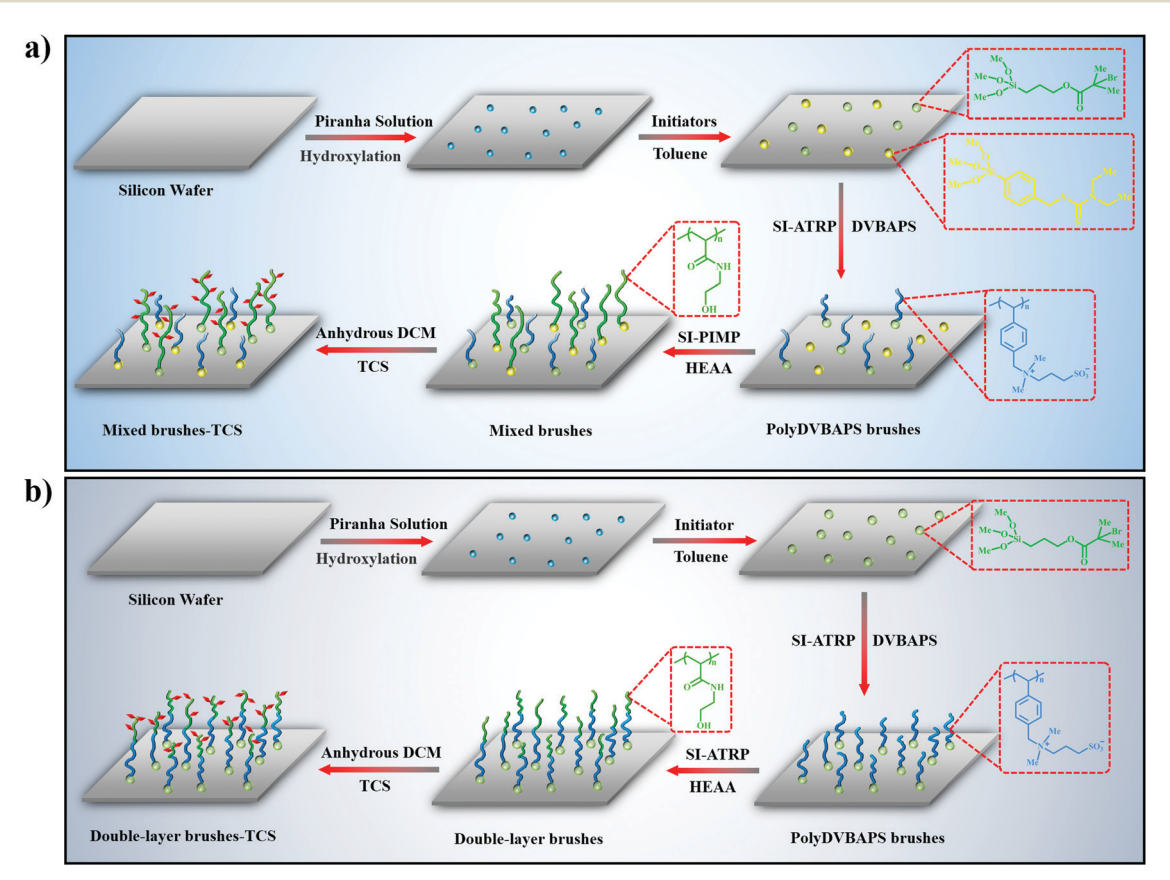
Cell cytotoxicity assay

L929 fibroblasts were incubated in Roswell Park Memorial Institute (RPMI) 1640 medium, supplemented with 1.0%

antibiotics (penicillin-streptomycin) and 10% fetal bovine serum by using a 5.0% CO₂ incubator at 37 °C. Then, 0.25% trypsin-EDTA solution was added to detach the adherent cells, re-dispersing the cell density at $\sim 5 \times 10^4$ cells per mL before incubating into a sterile culture medium. Subsequently, all samples (blank parallel replicates as controls included) were put into the cell suspension in a 24-well culture plate and incubated for 96 h. After that, the L929 cell solution was replaced by 1 mL of culture solution and 100 μL of MTT solution (5 mg mL $^{-1}$ in PBS) for another 4 h incubation. Finally, the mixtures were replaced by 1 mL of dimethyl sulfoxide (DMSO) to get the formazan solution by shaking for 10 min. The formazan solution was tested using a microplate reader (DG5033B, Huadong Electron Technology Co., Ltd, China) at a wavelength of 450 nm. The cell morphology of the L929 fibroblasts was observed on an Axio Observer A1 fluorescence microscope (Carl Zeiss Inc., Germany). All the samples were stained with 10 µL of FDA (Sigma) (5.0 µg mL⁻¹ in PBS) for 15 min in the dark, and then rinsed with sterile PBS solution before observing.

Results and discussion

Our previous works have demonstrated that polyDVBAPS possesses an excellent salt-responsive property to release



Scheme 1 Schematic of the two types of antibacterial polymer brushes with hierarchical structures of (a) a mixed polyDVBAPS/polyHEAA brush and (b) a double-layer poly(DVBAPS-b-HEAA) brush, both of which are covalently bonded to TCS.

attached bacteria from surfaces, 27,36,45,46 polyHEAA is a superlow fouling material to effectively resist the unwanted adsorption of proteins/cells/bacteria,40-42 and TCS is a well-known strong bactericide. 43,44 However, we have not realized the integration of these three components/materials together into a single surface for an antibacterial purpose. In this work, we presented two different surface-grafting strategies to prepare antibacterial polymer brushes with different hierarchical structures by polymerizing polyDVBAPS and polyHEAA in a different way. The first preparation strategy, as shown in Scheme 1a, is to sequentially graft polyDVBAPS using surface-initiated atom transfer radical polymerization (SI-ATRP) and polyHEAA using SI-PIM onto a silicon substrate, forming a mixed polyDVBAPS/ polyHEAA brush. By optimizing the molar ratio of ATRP initiator: PIMP initiator at 1:1 and the thickness of the polyDVBPAS brush at ~ 15 nm/ ~ 30 nm and the polyHEAA brush at ~ 35 nm, two

mixed polyDVBAPS/polyHEAA brushes were prepared for comparison. Due to the superlow fouling property of the polyHEAA brush, all polyDVBAPS/polyHEAA brushes were designed to have a relatively higher thickness of the polyHEAA brush than the polyDVBAPS brush in order to maintain the high antifouling property. Alternatively, we also applied a two-step ATRP to first graft a polyDVBAPS brush of $\sim 35~\rm nm$ on the silicon substrate as a supporting layer, followed by the copolymerization of polyHEAA onto the polyDVBAPS brush to form an additional thin layer of $\sim 10~\rm nm$, resulting in a double-layer brush (Scheme 1b). Upon the synthesis of both types of polyDVBAPS/polyHEAA and poly(DVBAPS-b-HEAA) brushes, TCS was then incorporated into polyHEAA chains via the condensation between acid chloride and hydroxyl groups. 39

Upon the grafting of the polymer brush onto the silicon substrate, XPS was used to characterize the composition of

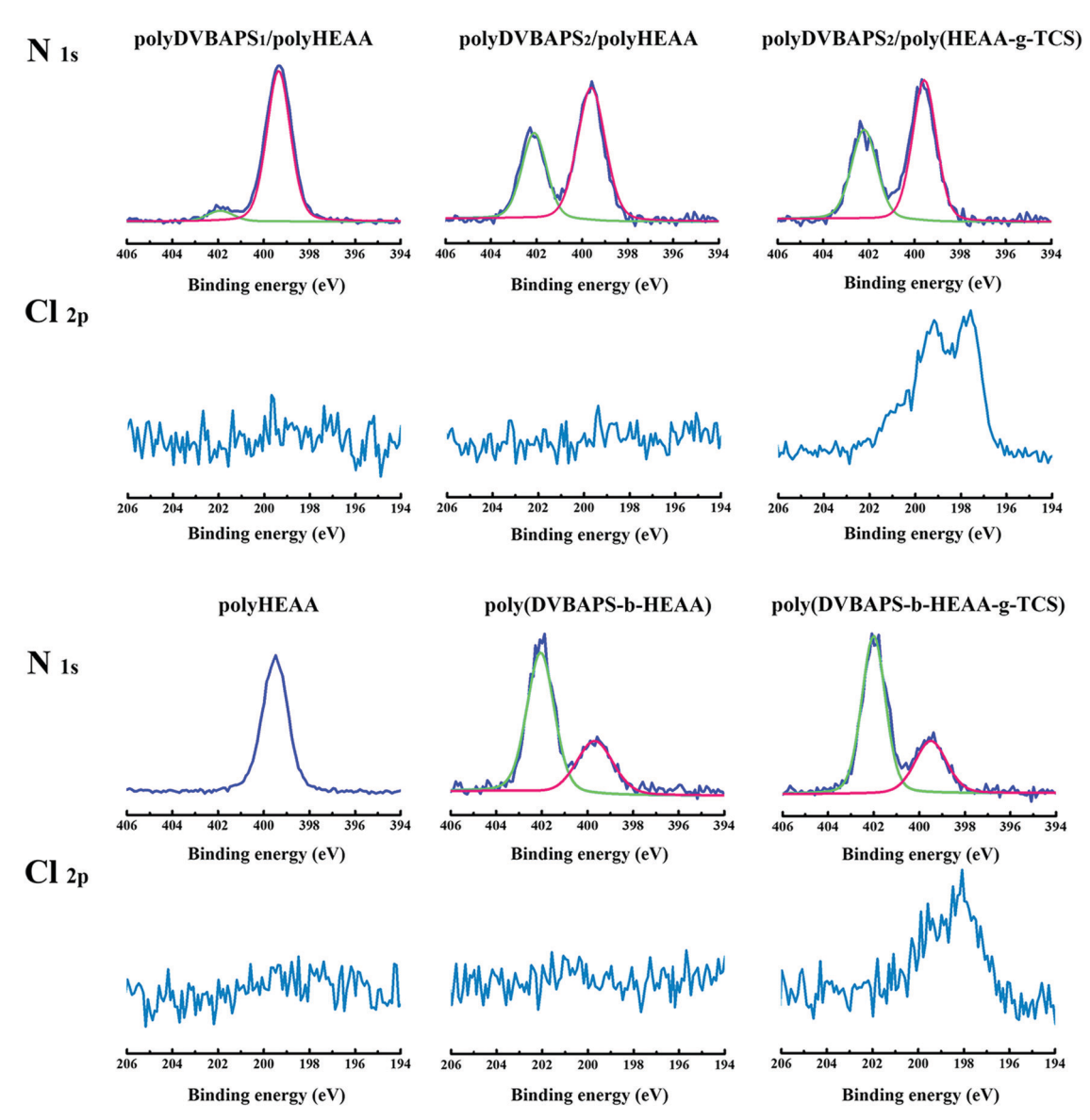


Fig. 1 XPS spectra obtained from N 1s and Cl 2p high-resolution survey scanning of polyDVBAPS $_1$ /polyHEAA, polyDVBAPS $_2$ /polyHEAA

brush-grafted surfaces and to confirm the successful polymerbrush coating. Both N 1s and Cl 2p high-resolution scans, as shown in Fig. 1, showed that both polyDVBAPS/polyHEAA and polyDVBAPS/poly(HEAA-g-TCS) brushes displayed a characteristic peak of polyHEAA at ~399.5 eV assigned to N(CH₃) and another distinct characteristic peak of pristine polyDVBAPS at ~402.2 eV assigned to N⁺(CH₃)₃, indicating the coexistence of polyHEAA and polyDVBAPS. However, different polymer brushes also exhibited different peak intensity ratios (the peak at ~ 402.2 eV vs. the peak at \sim 399.5 eV), reflecting the relative thickness difference between both polyHEAA and polyDVBAPS brushes. For example, for poly-DVBAPS/polyHEAA brushes, the increase of polyDVBAPS thickness led to a higher peak ratio. Differently, poly(DVBAPS-b-HEAA) brushes showed a higher peak at \sim 402.2 eV than that at \sim 399.5 eV due to a very thin polyHEAA layer. Further, upon grafting TCS on both polymer brushes, a new peak of Cl at ~198.2 eV was observed, corresponding to Cl 2p from TCS and indicating the successful introduction of the antibacterial agent. Based on the element percentage of Cl and N characterized from quantitative XPS measurements, the percentage of grafted TCS onto the brushes was calculated as 20 mol% for polyDVBAPS2/poly(HEAA-g-TCS) and 6.4 mol% for poly(DVBAPS-b-HEAA), respectively (Table 1).

Surface morphology of the polymer brush is of particular importance for its interactions with biomolecules. Generally speaking,

Table 1 Elemental percentage of C, N, and Cl in TCS-grafted brushes

| | Elemental mole percent (atom%) | | | |
|---|--------------------------------|-------|--------|-------------|
| Samples | C(1s) | N(1s) | Cl(2p) | HEAA/DVBAPS |
| PolyDVBAPS ₂ /poly(HEAA-g-TCS) | | | | 1.49 |
| Poly(DVBAPS-b-HEAA-g-TCS) | 89.98 | 9.41 | 0.61 | 0.45 |

a smooth surface not only reduces the possibility to kinetically trap bacteria, but also possesses a lower surface energy for surface resistance to bacteria. As shown in the tapping-mode AFM images (Fig. 2), all of the prepared brushes had very smooth surfaces with a low roughness of <1.7 nm. For comparison, the surface smoothness of polymer brushes exhibited a decreased order of pristine polyHEAA (RMS = 0.7 nm) < poly(DVBAPS-b-HEAA) (RMS = 1.2 nm) < polyDVBAPS/polyHEAA(RMS = 1.5 nm). These results also indicate that the SI-PIMP method appears to generate a higher surface roughness than the SI-ATRP method, probably due to the faster polymerization rate of polymer chains, consistent with our previous study.²⁷ Furthermore, by the grafting of antibacterial agents of TCS onto both poly(DVBAPS-b-HEAA) and polyDVBAPS/polyHEAA brushes, the surface roughness of poly(DVBAPS-b-HEAA-g-TCS) and poly-DVBAPS/poly(HEAA-g-TCS) was slightly increased by 0.22 nm and 0.04 nm, respectively, thus this did not affect the smooth topology of grafting polymer brushes for antibacterial tests.

Since surface resistance and release of bacteria are somehow related to surface wettability and the salt-responsive property of polymer brushes, Fig. 2c compares the contact angles of six different polymer brushes in water and salt solutions. As a control, a pristine polyHEAA brush showed a very low contact angle of $\sim 18.1^{\circ}$ in water and a much larger angle of $\sim 30.2^{\circ}$ in salt solution, indicating that the polyHEAA brush tends to change its surface wettability from very hydrophilic in water to more hydrophobic in salt solution. When the more hydrophobic DVBAPS was introduced to co-mix or co-polymerize with polyHEAA, both poly(DVBAPS-b-HEAA)- and polyDVBAPS/polyHEAAbased brushes not only slightly increased their contact angles, but also possessed salt-responsive surface wettability that exhibited a lower contact angle in salt solution than that in water.

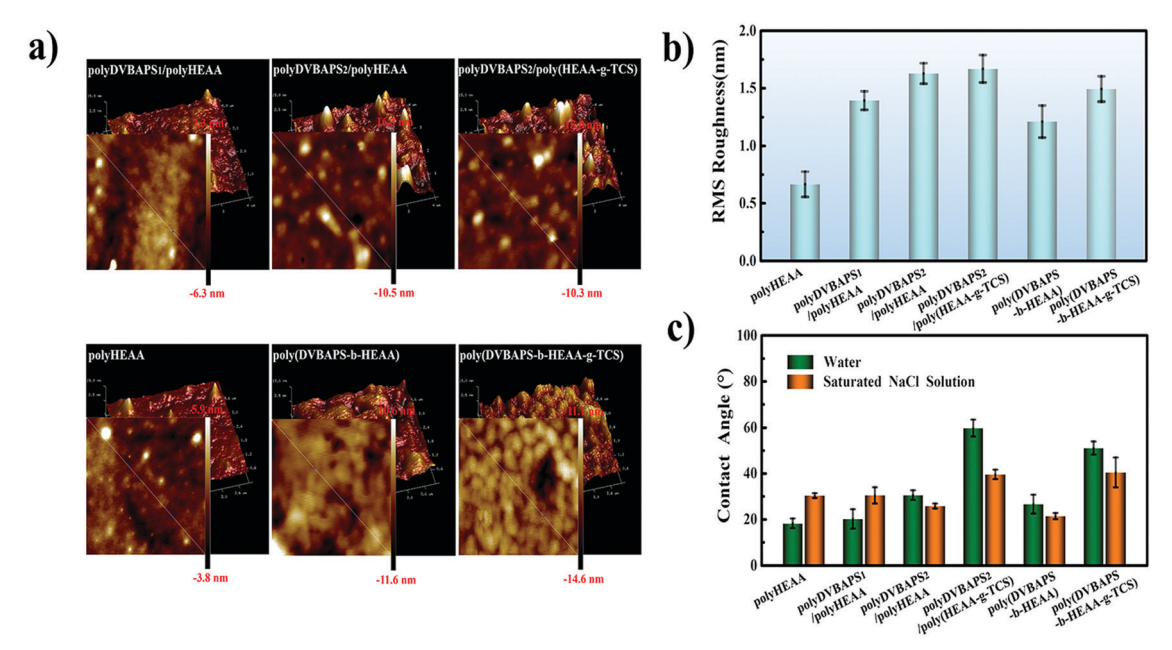


Fig. 2 (a) Representative AFM images (scan range = 4 μm), (b) RMS roughness, and (c) water contact angle for polyHEAA, polyDVBAPS₁/polyHEAA, polyDVBAPS2/polyHEAA, polyDVBAPS2/poly(HEAA-g-TCS), poly(DVBAPS-b-HEAA), and poly(DVBAPS-b-HEAA-g-TCS) brushes.

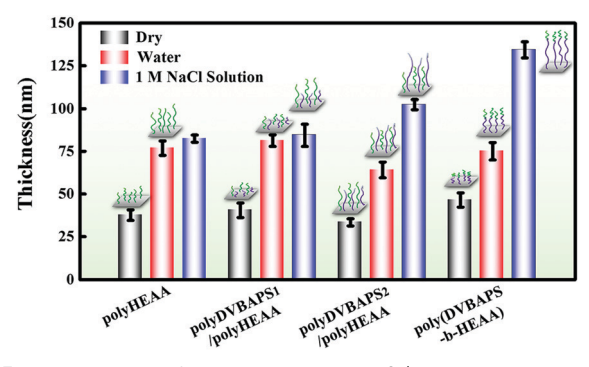


Fig. 3 Film thickness of polyHEAA, polyDVBAPS $_1$ /polyHEAA, polyDVBAPS $_2$ /polyHEAA, and poly(DVBAPS-b-HEAA) in a dry state, water solution, and 1 M NaCl solution.

Evidently, the poly(DABAPS-b-HEAA) brush decreased its contact angle from $\sim\!26.5^\circ$ in water to $\sim\!21.3^\circ$ in saturated salt solution, while the polyDVBAPS₂/polyHEAA brush decreased its contact angle from $\sim\!30.5^\circ$ in water to $\sim\!25.7^\circ$ in saturated salt solution. The grafting of TCS to both types of polymer brushes significantly increased the contact angles in both water and salt solutions due to the high hydrophobicity of TCS, but the salt-responsive surface wettability still remained to show the lower contact angle in salt solution.

Apart from salt-induced surface wettability, we further examined the salt-induced structural transformation of polymer brushes in different solvents, as measured by the change of film thickness in situ. Fig. 3 shows a side-by-side comparison of film thickness of the four polymer brushes in the dry, water solution, and salt solution states. As a control, the pure poly-HEAA brush exhibited a smaller thickness of \sim 37.6 nm in a dry state, but almost doubled its film thickness to \sim 76.9 nm in both water and salt solutions, indicating that the polyHEAA brush stretches its polymer chains due to strong hydrophilicity. Such chain stretching is independent of the solutions, consistent with the contact angle results. In the case of the polyDVBAPS/ polyHEAA brush, when the short polyDVBPAPS brush (~ 15 nm) was co-mixed with the polyHEAA brush, the trend of film thickness change from dry state (~ 40.4 nm) to water solution ~ 81.3 nm and to salt solution (\sim 84.3 nm) was similar to that of the pure polyHEAA brush. This is because of the fact that the polyDVBAPS brush in this case was very short and hidden in the polyHEAA brush, even though polyDVBAPS stretched its chains in water and salt solution. Consistently, for polyDVBAPS₂/polyHEAA with ~ 30 nm of polyDVBAPS and ~ 35 nm of polyHEAA, the salt solution led to a much higher thickness (~ 102.3 nm) than water (~64.1 nm), indicating that the highly stretched poly-DVBAPS chains in salt solution (\sim 3 times longer than dry brush thickness) could easily protrude from the polyHEAA layer. As expected, the poly(DVBAPS-b-HEAA) copolymer brush also exhibited excellent salt-responsive structural transformation, as evidenced by an increase of film thickness from \sim 46.5 nm in the dry state to \sim 75.1 nm in water solution and to \sim 134.3 nm in salt solution.

Upon demonstrating the salt-induced surface property changes of two types of polymer brushes, we further investigated the overall

antibacterial performance of these brushes (including bacterial resistance, killing, and release) using Escherichia coli (E. coli, Gramnegative) and Staphylococcus aureus (S. aureus, Gram-positive). First, we examined the antibacterial performance of poly-DVBAPS/polyHEAA-based brushes using E. coli, and Fig. 4a and b show the fluorescence microscopy images and the corresponding statistical results of E. coli accumulation on different polyDVBAPS/polyHEAA-based brushes for 120 h. Both visual inspection and data analysis showed that with the increase of culture time, the number of adherent E. coli on all polymer brushes increased linearly. Upon 5 day incubation of E. coli with the four polymer brushes, the adhered bacterial amount on polymer brushes exhibited an increasing order of $\sim 20.0 \times 10^4$ cells per cm² on the pure polyHEAA brush $< \sim 35.3 \times 10^4$ cells per cm² on the polyDVABAPS₁/polyHEAA brush $< \sim 54.9 \times 10^4$ cells per cm² on the polyDVBAPS₂/ polyHEAA brush. Among them, the pure polyHEAA brush exhibited the highest surface resistance to E. coli, while the mixed polyDVBAPS/polyHEAA brushes showed decreased antifouling property to some extent presumably due to the more hydrophobic nature of the polyDVBAPS brush. 45,46 As compared to the unmodified surface that absorbed a large amount of bacteria quickly ($\sim 84.3 \times 10^4$ cells per cm² for 24 h), as shown in Fig. S1 (ESI†), all these polymer brushes are considered as effective antifouling surfaces based on an antibacterial density criterion of $< \sim 10^6$ cells per cm².

Next, we continued to test the bacterial release capacity of the four bacteria-attached polymer brushes by immersing the brushes into 1 M salt solution for 15 min and rinsing with PBS solution. Fig. 4c shows the comparison of the resultant attached bacterial density before and after salt treatment. It can be seen that while the polyHEAA brush showed the best antifouling property to resist bacterial attachment, salt-treatment only released ~31.8% of the attached bacteria, indicating a poor bacterial release capacity of the polyHEAA brush. For the mixed polyDVBAPS/polyHEAA brushes, the presence of polyDVBAPS is expected to endow the brushes with bacterial release capability. So, upon salt-solution treatment, the polyDVBAPS₁/polyHEAA brush with a thin polyDVBAPS₁ brush (~ 15 nm) released $\sim 52.8\%$ of the attached bacteria, showing a moderate bacterial release capability. A further increase of polyDVBAPS brush thickness to ~ 30 nm significantly improved bacterial release capacity, leading to \sim 87.5% of the attached bacteria being released. This indicates a strong thickness dependence of the polyDVBAPS brush on the bacterial release capacity of polyDVBAPS/polyHEAA brushes, i.e., upon salt treatment, salt-responsive polyDVBAPAS chains will stretch out from a polyHEAA brush to realize high bacterial release capability.

To further demonstrate the bacterial killing property, we grafted a bactericidal agent of TCS onto polyHEAA chains to form a polyDVBAPS₂/poly(HEAA-g-TCS) brush. Visual inspection of Fig. 4a again showed that the presence of TCS in the polyDVBAPS₂/poly(HEAA-g-TCS) brush killed almost all attached bacteria, as evidenced by the red-colored dead bacteria in the fluorescent images. In addition, the polyDVBAPS₂/poly(HEAA-g-TCS) brush further reduced the attached bacterial density to $\sim 23.0 \times 10^4$ cells per cm², as compared to $\sim 54.9 \times 10^4$ cells per cm² on the

Against E. coli

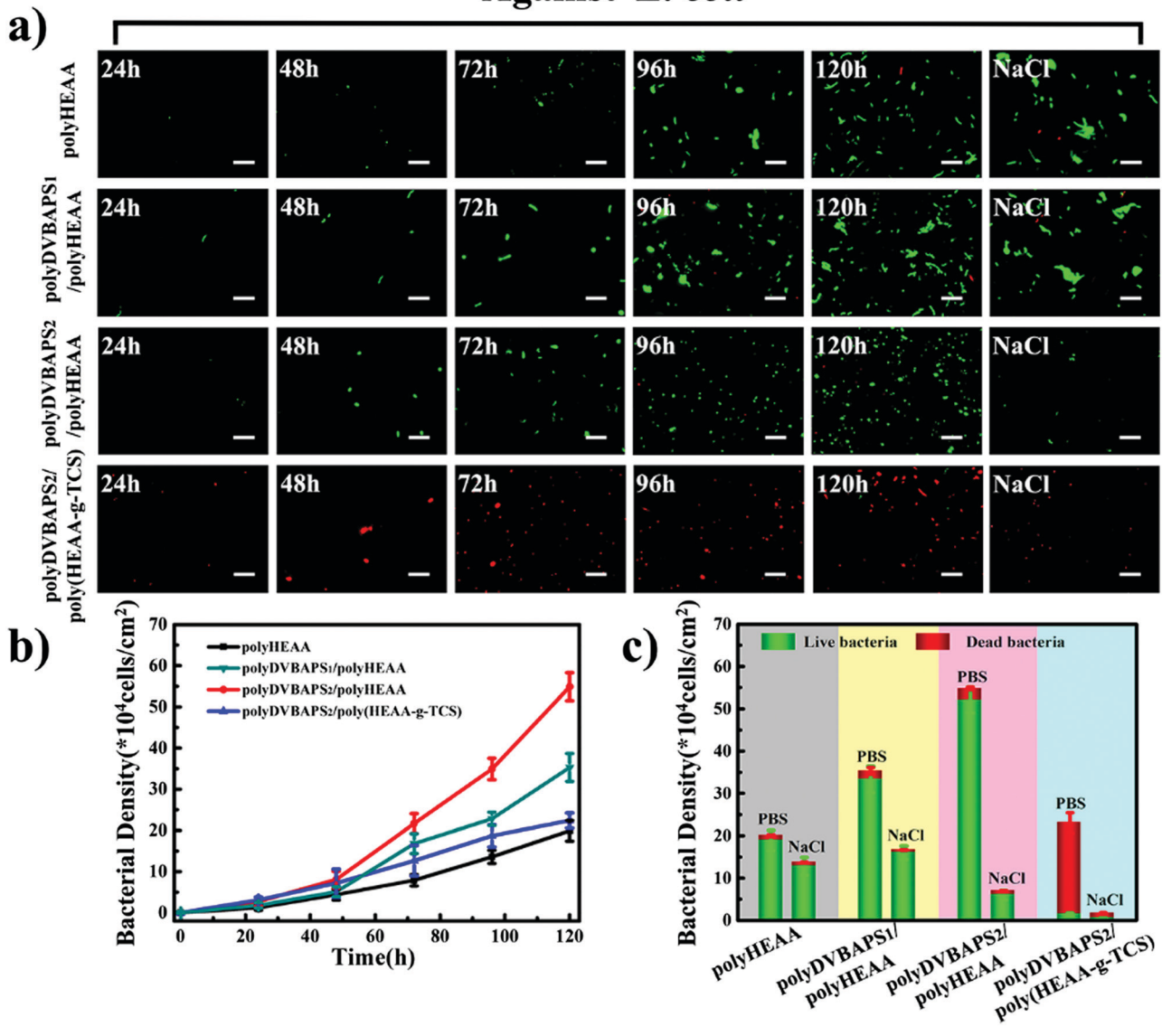


Fig. 4 Overall antibacterial performance contributed by bacterial resistance, killing, and release of polyDVBAPS/polyHEAA-based brushes using E. coli. (a) Representative fluorescence microscopy images (scale bar is 20 µm) and (b) the corresponding statistical results of E. coli accumulation on polyHEAA, $polyDVBAPS_1/polyHEAA,\ polyDVBAPS_2/polyHEAA,\ and\ polyDVBAPS_2/poly(HEAA-g-TCS)\ brushes\ at\ different\ incubation\ times.\ (c)\ Comparison\ of\ polyDVBAPS_2/polyHEAA,\ polyDVBAPS_2/polyHEAA,\$ bacterial density before and after the treatment of 1.0 M NaCl solution to determine the bacterial release ratio. Similar antibacterial performance of polyDVBAPS/polyHEAA-based brushes using S. aureus is shown in Fig. S2 (ESI†).

polyDVBAPS₂/polyHEAA brush without TCS. Such a decrease of bacterial density on the brush is likely attributed to the contact killing capacity of the brush.³⁶ More importantly, the bacterial release property was still well retained, and upon salt-solution treatment, the attached bacterial density was further significantly reduced to $\sim 1.6 \times 10^4$ cells per cm², releasing $\sim 93.0\%$ attached bacteria. In parallel, we also used the S. aureus bacterial assay to confirm the general antibacterial property of polyDVBAPS/polyHEAA-based brushes. As expected, polyDVBAPS₂/poly(HEAA-g-TCS) brushes showed excellent bacterial resistance, bactericidal activity, and bacterial release properties, as indicated by a low attached bacterial density of $\sim 31.8 \times 10^4$ cells per cm², a high bacterial killing efficiency of $\sim 97.4\%$, and a large salt-induced bacterial release of \sim 94.3% (Fig. S2, ESI†).

Next, we tested the surface regeneration capacity of poly-DVBAPS₂/polyHEAA and polyDVBAPS₂/poly(HEAA-TCS) brushes with and without TCS to determine whether the brushes could still retain their antifouling, bactericidal, and bacterial release properties using three cycles of two different bacterial assays, where each cycle includes 15 day incubation with E. coli and 9 day incubation with S. aureus. We used different incubation times for different bacteria, simply because of the different proliferation rates of the bacteria to achieve a cut-off value of 10⁶ bacteria per cm². Since S. aureus achieved this value faster than E. coli due to the higher proliferation rate and attachment tendency, a shorter incubation time of 9 days was used for *S. aureus*. In Fig. 5a and b, after each "antifouling-killing-release" cycle, the polyDVBAPS₂/polyHEAA brush did not show obvious changes in both *E coli* and *S. aureus* attachment ($\sim 0.25 \times 10^6$ cells per cm² and $\sim 0.3 \times 10^6$ cells per cm², respectively), indicating that the salt-induced surface regeneration is able to retain its bacterial resistance, killing, and release functions, and thus achieves almost the same antibacterial performance as that in the first cycle. Specifically, during the three cycles, the attached bacterial density remained almost unchanged, as indicated by values of $\sim 23.0 \times 10^4$ cells per cm²,

 $\sim\!26.9\times10^4$ cells per cm², and $\sim\!31.0\times10^4$ cells per cm² for *E. coli*, and $\sim\!32.0\times10^4$ cells per cm², $\sim\!30.2\times10^4$ cells per cm², and $\sim\!38.1\times10^4$ cells per cm² for *S. aureus*, respectively (Fig. 5a and b). Meanwhile, polyDVBAPS₂/poly(HEAA-g-TCS) also showed high bactericidal activity to kill $\sim\!93.0\%$, $\sim\!94.8\%$, and $\sim\!93.1\%$ *E. coli* and $\sim\!97.4\%$, $\sim\!95.4\%$, and $\sim\!94.3\%$ *S. aureus*, respectively (Fig. 5c). Upon salt-solution treatment, the polyDVBAPS₂/poly(HEAA-g-TCS) brush showed a consistent bacterial release of $\sim\!90.2\%$, $\sim\!91.5\%$, and $\sim\!89.0\%$ for *E. coli* and $\sim\!94.3\%$, $\sim\!89.7\%$, and $\sim\!92.4\%$ for *S. aureus* during the three cycles. Thus, the polyDVBAPS₂/poly(HEAA-g-TCS) brush

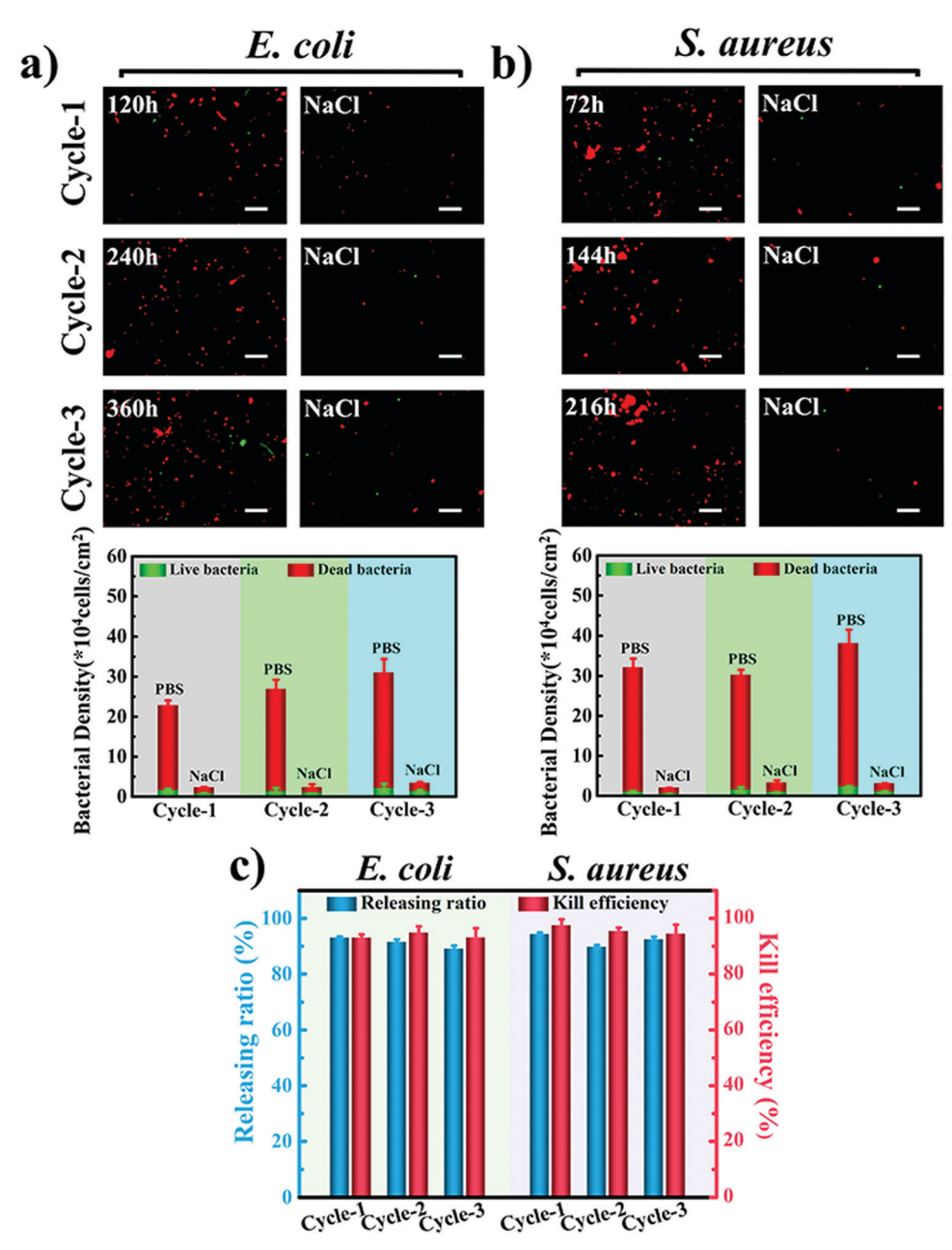


Fig. 5 Overall antibacterial performance contributed by antifouling, bactericidal, and bacterial release properties and the salt-induced surface regeneration of the polyDVBAPS $_2$ /poly(HEAA-g-TCS) brush in multiple and reversible cycles, as evidenced by fluorescence microscopy images (scale bar = 20 μ m) and the corresponding live/dead cell analysis for (a) *E. coli* and (b) *S. aureus*. (c) Cyclic bacterial killing and release of polyDVBAPS $_2$ /poly(HEAA-g-TCS) brushes against *E. coli* and *S. aureus* upon the treatment of 1.0 M NaCl solution.

is able to achieve and maintain the long-term, tri-functional antibacterial property via surface regeneration for up to 15 days for E. coli and 9 days for S. aureus. For comparison, in the case of the polyDVBAPS₂/polyHEAA brush without TCS, Fig. S3 (ESI†) shows that for each "antifouling-release" cycle, while the poly-DVBAPS₂/polyHEAA brush did not show obvious changes in both E. coli and S. aureus attachment ($\sim 0.58 \times 10^6$ cells per cm² and $\sim 0.61 \times 10^6$ cells per cm², respectively), the attached bacterial density was much higher than that on the polyDVBAPS₂/ poly(HEAA-g-TCS) brush. Upon salt-solution treatment, the bacterial release efficiency the of three cycles was $\sim 87.5\%$, $\sim 85.0\%$, and

 $\sim 80.0\%$ for *E. coli*, and $\sim 88.4\%$, $\sim 85.6\%$, and $\sim 82.3\%$ for S. aureus, respectively. The slight decrease of bacterial release capability with cycles could be due to the irreversible absorption of small debris. Clearly, the lack of TCS to kill bacterial capacity renders a lower antibacterial efficiency of polyDVBAPS2/polyHEAA brushes. Even worse, polyHEAA brushes, due to the lack of both bacterial killing-and-release capacity, eventually lost their initial antifouling property to induce a large adsorption number of bacteria up to 9 day incubation ($\sim 1.0 \times 10^6$ cells per cm², Fig. S4, ESI†). As compared to the poly(DVBAPS) brush without TCS, the poly(DVBAPS) brush with TCS can significantly reduce the number

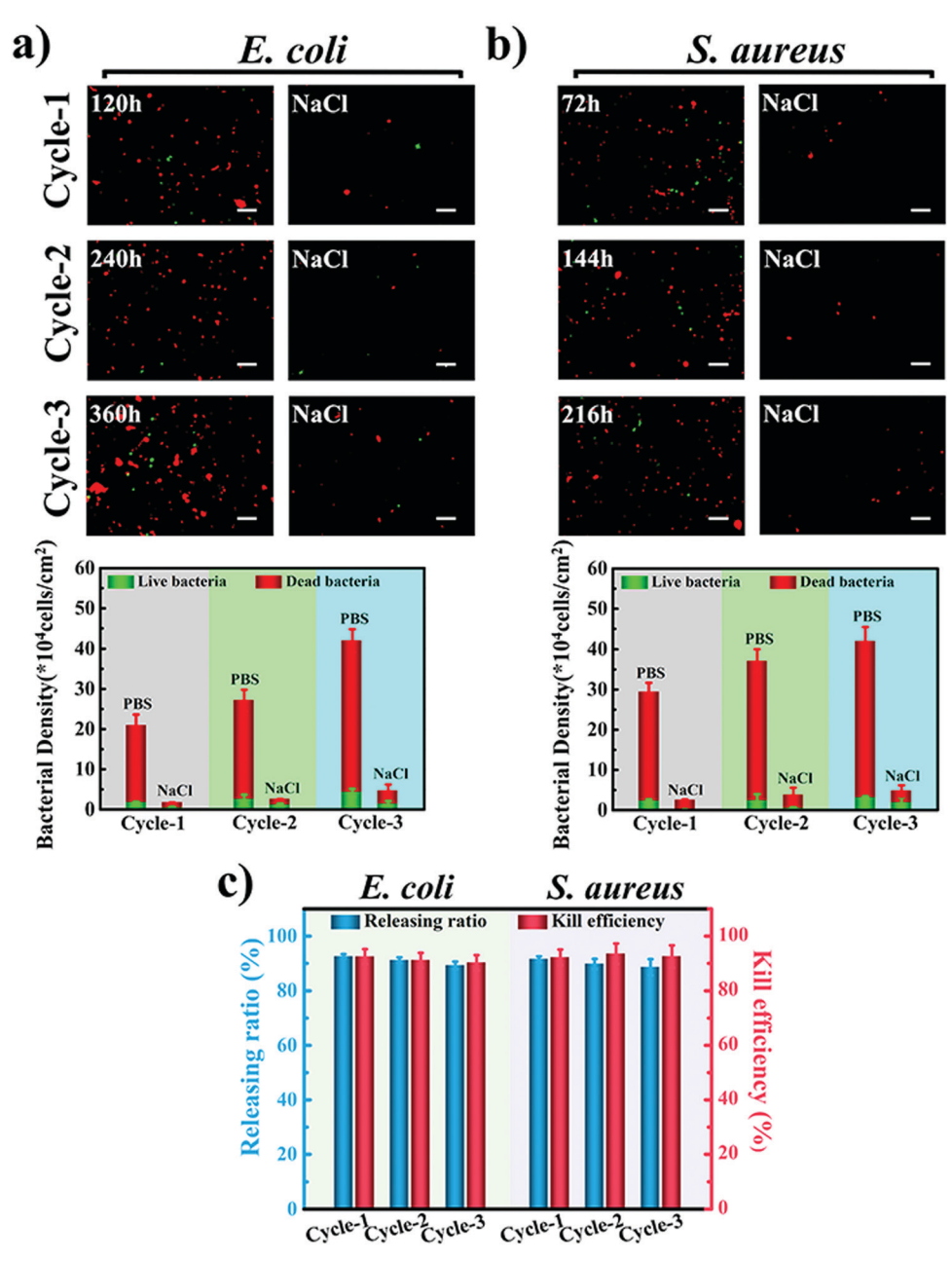


Fig. 6 Overall antibacterial performance contributed by antifouling, bactericidal, and bacterial release properties and the salt-induced surface regeneration of the poly(DVBAPS-b-HEAA-q-TCS) brush in multiple and reversible cycles, as evidenced by fluorescence microscopy images (scale bar = 20 µm) and the corresponding live/dead cell analysis for (a) E. coli and (b) S. aureus. (c) Cyclic bacterial killing and release of the poly(DVBAPS-b-HEAA-g-TCS) brush against E. coli and S. aureus upon the treatment of 1.0 M NaCl solution.

of attached bacteria, particularly live bacteria. Therefore, both effects will largely maintain the bacterial release capability of the poly(DVBAPS) brush with TCS, because dead bacteria and less bacteria are more easily released than live bacteria and more bacteria. Thus, comparison of polyDVBAPS2/poly(HEAA-g-TCS), polyDVBAPS₂/polyHEAA, and polyHEAA demonstrates our design strategy to integrate bacterial resistance, killing, and release properties into single materials for improving the overall antibacterial performance. Of note, we carefully characterized the surface using AFM and ellipsometry by testing the morphology and thickness at different positions, and no obvious uncoated area was found, presumably because the SI-ATRP method is a well-known and mature coating technology for surface engineering that can readily and completely cover the whole underlying surface with polymer brushes, except for only one condition that the covered polymer brush is very thin, which has been eliminated in our study by using the optimal and thick polymer brushes.

Following the same experimental protocols and tests, we continuously examined the long-term bacterial resistance, killing, and release properties of poly(DVBAPS-b-HEAA-g-TCS) brushes in multiple surface regenerative cycles using both E. coli and S. aureus, in comparison with the poly(DVBAPS-b-HEAA) brush without TCS. Due to the good regenerative properties, poly(DVBAPS-b-HEAA) showed excellent antifouling and bacterial release properties in three cycles, albeit a slight decrease in both killing and release properties was observed with the increase of cycles. After three cycles, the antifouling properties were well retained at ultralow fouling levels of $\sim 56.7 \times 10^4$ cells per cm² and $\sim 73.2 \times 10^4$ cells per cm², and bacteria release capabilities were also retained at high levels of \sim 89.3% and \sim 88.6% for *E. coli* and S. aureus, respectively (Fig. S5, ESI†). But without TCS, the poly(DVBAPS-b-HEAA) brush showed very slight bactericidal activity. For poly(DVBAPS-b-HEAA-g-TCS) brushes, as shown in Fig. 6, during the three "antifouling, killing, and release" cycles, the density of bacteria attached on the poly(DVBAPS-b-HEAA-g-TCS) brush between any two cycles remained almost unchanged for E. coli ($\sim 41.9 \times 10^4$ cells per cm²) and S. aureus $(\sim 42.1 \times 10^4 \text{ cells per cm}^2)$, respectively, both of which were significantly lower than the attached density of E. coli (\sim 56.7 \times 10^4 cells per cm²) and S. aureus ($\sim 73.2 \times 10^4$ cells per cm²) on the poly(DVBAPS-b-HEAA) brush without TCS (Fig. S5, ESI†). Moreover, the poly(DVBAPS-b-HEAA-g-TCS) brush was able to kill $\sim 92.4\%$ (cycle 1), $\sim 91.2\%$ (cycle 2), $\sim 90.2\%$ (cycle 3) E. coli, and \sim 92.2% (cycle 1), \sim 93.5% (cycle 2), \sim 92.5% (cycle 3) S. aureus (Fig. 6c). Finally, the salt-induced surface regeneration enabled the release of $\sim 92.6\%$ (cycle 1), $\sim 91.2\%$ (cycle 2), and \sim 89.3% (cycle 3) *E. coli*, and \sim 91.6% (cycle 1), \sim 89.8% (cycle 2), and 88.6% (cycle 3) S. aureus, respectively. Poly(DVBAPS-b-HEAA) block brushes exhibited a higher antifouling capability than poly-DVBAPS/polyHEAA brushes, due to a higher surface coverage by polyHEAA. Taken together, the copolymerized poly(DVBAPS-b-HEAA-g-TCS) brush displayed similar antibacterial performance to the mixed polyDVBAPS₂/poly(HEAA-g-TCS) brush, demonstrating a general working strategy to improve antibacterial performance by integrating three bacterial resistance, killing, and release properties into a single material.

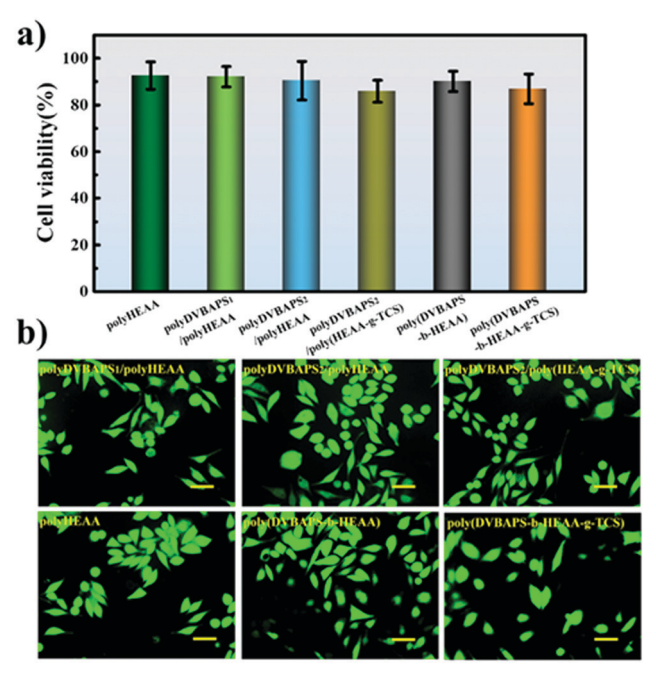


Fig. 7 (a) Cell viability assay and (b) representative fluorescent microscopy images of L929 fibroblasts cultured with polyHEAA, polyDVBAPS₁/polyHEAA, polyDVBAPS₂/polyHEAA, polyDVBAPS₂/poly(HEAA-*g*-TCS), poly(DVBAPS-*b*-HEAA) and poly(DVBAPS-*b*-HEAA-*q*-TCS) brushes for 96 h. Scale bar = 50 µm.

Cytocompatibility including cytotoxicity and the adhesion and growth of normal cells on surfaces is another important factor for the design of effective antibacterial surfaces. Here, we examined the cytocompatibility of the six brushes of polyHEAA, polyDVBAPS₁/polyHEAA, polyDVBAPS₂/polyHEAA, polyDVBAPS₂/ poly(HEAA-g-TCS), poly(DVBAPS-b-HEAA) and poly(DVBAPS-b-HEAA-g-TCS) using MTT assay with a L929 fibroblast cell line. The morphology and viability of L929 cells on polystyrene surfaces after 96 h incubation were used as controls. Fig. 7a shows that after 96 h incubation with cells, all the polymer brushes exhibited an excellent cell viability of 85-93%. As compared to polymer brushes without TCS, TCS-incorporated polymer brushes only reduced cell viability by $\sim 5\%$. While visual inspection also confirmed that the cell density on all polymer brushes increased with time, cells attached on polymer brushes with and without TCS displayed different morphologies (Fig. 7b), i.e., the cells on pure polyHEAA, polyDVBAPS₁/polyHEAA, polyDVBAPS₂/polyHEAA, and poly(DVBAPS-b-HEAA) brushes showed an unfurled lamellar shape, indicating a healthy growth and proliferation state. Differently, some cells on TCS-incorporated polymer brushes adapted their morphologies to round-like shapes, thus reducing cell viability to a small extent, consistent with MTT results. Overall, polyDVBAPS₂/polyHEAA and poly(DVBAPS-b-HEAA) brushes demonstrated their good cytocompatibility to promote cell adhesion and proliferation.

Conclusions

In this work, we proposed a new design strategy to fabricate tri-functional and regenerable antibacterial surfaces by polymerizing and grafting salt-responsive polyDVBAPS, antifouling polyHEAA, and bactericidal TCS on a substrate to form mixed polyDVBAPS/ poly(HEAA-g-TCS) and double-layer poly(DVBAPS-b-HEAA-g-TCS) brushes. Both polymer brushes of different topological structures were characterized and confirmed for their surface composition, surface morphology, and chain conformation by XPS, AFM, and ellipsometry. The resultant polymer brushes were further tested using Escherichia coli (E. coli, Gram-negative) and Staphylococcus aureus (S. aureus, Gram-positive) to demonstrate their triantibacterial activities of long-term surface resistance to bacteria at an ultralow fouling level ($\sim 10^6$ cells per cm²) for 5 days, strong bactericidal activity to kill more than $\sim 90\%$ attached bacteria, and high salt-responsive surface regeneration capacity for releasing $\sim 90\%$ attached bacteria. More importantly, both mixed and double-layer polymer brushes can be easily regenerated for reuse by treatment with NaCl solution, so that the overall antibacterial performance was well retained after several "antifouling-killing-release" cycles, where each cycle includes a 15 day incubation with E. coli and 9 day incubation with S. aureus. Practically, no antifouling surface or coating can permanently sustain its antifouling property for a long-term period, i.e., as time proceeds, there are always some foulants that adsorb or accumulate onto the surfaces. Even 5 ng cm⁻² protein adsorption will eventually trigger biofilm formation. From a design viewpoint, antifouling surfaces have been designed to possess multiple functions, starting from pure surface resistance property, to a combination of surface resistance and contact killing properties, to the probably most promising combination of surface resistance, contact killing, and bacterial release properties. Thus, our design strategy and polymer systems offer a promising way to fabricate multifunctional and regenerable antibacterial surfaces for different antibacterial applications.

Conflicts of interest

There are no conflicts to declare.

Acknowledgements

J. Y. acknowledges the financial support from the Natural Science Foundation of China (No. 51673175), the Natural Science Foundation of Zhejiang Province (LY16E030012), and the Zhejiang Top Priority Discipline of Textile Science and Engineering (2015KF06). J. Z. acknowledges the financial support from the NSF (DMR-1806138).

References

- 1 L. Hall-Stoodley, J. W. Costerton and P. Stoodley, Bacterial biofilms: from the Natural environment to infectious diseases, *Nat. Rev. Microbiol.*, 2004, 2, 95–108.
- 2 J. W. Costerton, P. S. Stewart and E. P. Greenberg, Bacterial biofilms: a common cause of persistent infections, *Science*, 1999, **284**, 1318–1322.

- 3 R. T. Katie, M. Anne, G. Denise, E. Joanne, L. S. Nicole, J. Lynn, S. Kathryn, E. John, H. Elizabeth and J. Michael, A point prevalence survey of health care-associated infections in Canadian pediatric inpatients, *Am. J. Infect. Control*, 2012, 40, 491–496.
- 4 B. Allegranzi, N. S. Bagheri, C. Combescure, W. Graafmans, H. Attar, L. Donaldson and D. Pittet, Burden of endemic health-care-associated infection in developing countries: systematic review and meta-analysis, *Lancet*, 2011, 377, 228–241.
- 5 C. R. Arciola, D. Campoccia, P. Speziale, L. Montanaro and J. W. Costerton, Biofilm formation in Staphylococcus implant infections. A review of molecular mechanisms and implications for biofilm-resistant materials, *Biomaterials*, 2012, 33, 5967–5982.
- 6 P. A. Mak, S. P. Rao, T. M. Ping, X. Lin, J. Chyba, J. Tay, S. H. Ng, B. H. Tan, J. Cherian and J. Duraiswamy, A high-throughput screen to identify inhibitors of ATP homeostasis in non-replicating Mycobacterium tuberculosis, *ACS Chem. Biol.*, 2012, 7, 1190–1197.
- 7 R. M. Klevens, J. R. Edwards, C. L. Richards, T. C. Horan, R. P. Gaynes, D. A. Pollock and D. M. Cardo, Estimating Health Care-Associated Infections and Deaths in US Hospitals, 2002, *Public Health Rep.*, 2007, 122, 160–166.
- 8 E. M. Hetrick and M. H. Schoenfisch, Reducing implantrelated infections: active release strategies, *Chem. Soc. Rev.*, 2006, 35, 780–789.
- 9 F. Chen, S. Lu, L. Zhu, Z. Tang, Q. Wang, G. Qin, J. Yang, G. Sun, Q. Zhang and Q. Chen, Conductive regenerated silk-fibroin-based hydrogels with integrated high mechanical performances, *J. Mater. Chem. B*, 2019, 7, 1708–1715.
- 10 S. Mario, Q. Yue, G. James, R. A. Strugnell, L. Trevor, K. M. Mclean and T. Helmut, Emerging rules for effective antimicrobial coatings, *Trends Biotechnol.*, 2014, 32, 82–90.
- 11 Z. Tang, Q. Chen, F. Chen, L. Zhu, S. Lu, B. Ren, Y. Zhang, J. Yang and J. Zheng, General Principle for Fabricating Natural Globular Protein-Based Double-Network Hydrogels with Integrated Highly Mechanical Properties and Surface Adhesion on Solid Surfaces, Chem. Mater., 2018, 31, 179–189.
- 12 O. Ciofu, E. Rojo-Molinero, M. D. Macià and A. Oliver, Antibiotic treatment of biofilm infections, *APMIS*, 2017, **125**, 304–319.
- 13 M. Mccann and B. Gilmore, Sp, Staphylococcus epidermidis device-related infections: pathogenesis and clinical management, *J. Pharm. Pharmacol.*, 2010, **60**, 1551–1571.
- 14 B. Wang, Q. Xu, Z. Ye, H. Liu, Q. Lin, K. Nan, Y. Li, Y. Wang, L. Qi and H. Chen, Copolymer Brushes with Temperature-Triggered, Reversibly Switchable Bactericidal and Antifouling Properties for Biomaterial Surfaces, ACS Appl. Mater. Interfaces, 2016, 8, 27207–27217.
- 15 W. Zhan, T. Wei, L. Cao, C. Hu and H. Chen, Supramolecular Platform with Switchable Multivalent Affinity: Photo-Reversible Capture and Release of Bacteria, *ACS Appl. Mater. Interfaces*, 2017, **9**, 3505–3513.
- 16 X. Wei, J. Shen, Z. Gu, Y. Zhu, F. Chen, M. Zhong, L. Yin, Y. Xie, Z. Liu and W. Jin, Bioinspired pH-sensitive surface on bioinert substrate, ACS Appl. Bio Mater., 2018, 1, 2167–2175.
- 17 Y. Zhu, J. Shen, L. Yin, X. Wei, F. Chen, M. Zhong, Z. Gu, Y. Xie, W. Jin and Z. Liu, Directly photopatterning of polycaprolactone-derived photocured resin by UV-initiated thiol–ene "click"

- reaction: Enhanced mechanical property and excellent biocompatibility, *Chem. Eng. J.*, 2019, **366**, 112–122.
- 18 S. E. Kim, C. Zhang, A. A. Advincula, E. Baer and J. K. Pokorski, Protein and Bacterial Antifouling Behavior of Melt-Coextruded Nanofiber Mats, ACS Appl. Mater. Interfaces, 2016, 8, 8928–8938.
- 19 L. S. Wang, A. Gupta, B. Duncan, R. Ramanathan, M. Yazdani and V. M. Rotello, Biocidal and Antifouling Chlorinated Protein Films, ACS Biomater. Sci. Eng., 2016, 2, 1862–1866.
- 20 Z. K. Zander and M. L. Becker, Antimicrobial and Antifouling Strategies for Polymeric Medical Devices, ACS Macro Lett., 2018, 7, 16–25.
- 21 X. Fan, M. Hu, Z. Qin, J. Wang, X. Chen, W. Lei, W. Ye, Q. Jin, K. F. Ren and J. Ji, Bactericidal and Hemocompatible Coating via the Mixed-charged Copolymer, *ACS Appl. Mater. Interfaces*, 2018, **10**, 10428–10436.
- 22 S. Yan, S. Luan, H. Shi, X. Xu, J. Zhang, S. Yuan, Y. Yang and J. Yin, Hierarchical Polymer Brushes with Dominant Antibacterial Mechanisms Switching from Bactericidal to Bacteria Repellent, *Biomacromolecules*, 2016, 17, 1696–1704.
- 23 A. Perez-Anes, A. Szarpak-Jankowska, D. Jary and R. Auzely-Velty, β-CD-Functionalized Microdevice for Rapid Capture and Release of Bacteria, *ACS Appl. Mater. Interfaces*, 2017, 9, 13928–13938.
- 24 Z. Iryna, J. Freneil, A. B. Attygalle, W. Yong, M. R. Libera and S. A. Sukhishvili, Self-defensive layer-by-layer films with bacteriatriggered antibiotic release, ACS Nano, 2014, 8, 7733–7745.
- 25 T. Wei, W. Zhan, Q. Yu and H. Chen, Smart Biointerface with Photoswitched Functions between Bactericidal Activity and Bacteria-Releasing Ability, *ACS Appl. Mater. Interfaces*, 2017, 9, 25767–25774.
- 26 Q. Yu, J. Cho, P. Shivapooja, L. K. Ista and G. P. López, Nanopatterned smart polymer surfaces for controlled attachment, killing, and release of bacteria, ACS Appl. Mater. Interfaces, 2013, 5, 9295–9304.
- 27 Y. Fu, W. Yang, H. Lei, S. Xiao and J. Yang, Salt-Responsive "Killing and Release" Antibacterial Surfaces of Mixed Polymer Brushes, *Ind. Eng. Chem. Res.*, 2018, 57, 8938–8945.
- 28 Z. Wei, C. Wei, Z. Eric, B. E. Avraham, L. Xinglin, E. Menachem and B. Roy, Functionalization of ultrafiltration membrane with polyampholyte hydrogel and graphene oxide to achieve dual antifouling and antibacterial properties, *J. Membr. Sci.*, 2018, 565, 293–302.
- 29 T. Ren, M. Yang, K. Wang, Y. Zhang and J. He, CuO Nanoparticles-Containing Highly Transparent and Superhydrophobic Coatings with Extremely Low Bacterial Adhesion and Excellent Bactericidal Property, ACS Appl. Mater. Interfaces, 2018, 10, 25717–25725.
- 30 Z. Q. Shi, Y. T. Cai, J. Deng, W. F. Zhao and C. S. Zhao, Host-Guest Self-Assembly Toward Reversible Thermoresponsive Switching for Bacteria Killing and Detachment, ACS Appl. Mater. Interfaces, 2016, 8, 23523–23532.
- 31 B. Wang, Z. Ye, Q. Xu, H. Liu, Q. Lin, H. Chen and K. Nan, Construction of a temperature-responsive terpolymer coating with recyclable bactericidal and self-cleaning antimicrobial properties, *Biomater. Sci.*, 2016, 4, 1731–1741.

- 32 T. Wei, Q. Yu, W. Zhan and H. Chen, A Smart Antibacterial Surface for the On-Demand Killing and Releasing of Bacteria, *Adv. Healthcare Mater.*, 2016, 5, 449–456.
- 33 T. Wei, Z. C. Tang, Q. Yu and H. Chen, Smart Antibacterial Surfaces with Switchable Bacteria-Killing and Bacteria-Releasing Capabilities, *ACS Appl. Mater. Interfaces*, 2017, 9, 37511–37523.
- 34 T. Wei, Q. Yu and H. Chen, Responsive and Synergistic Antibacterial Coatings: Fighting against Bacteria in a Smart and Effective Way, *Adv. Healthcare Mater.*, 2019, **8**, 1801381.
- 35 W. J. Zhan, T. Wei, Q. Yu and H. Chen, Fabrication of Supramolecular Bioactive Surfaces *via* β-Cyclodextrin-Based Host-Guest Interactions, *ACS Appl. Mater. Interfaces*, 2018, **10**, 36585–36601.
- 36 D. Zhang, Y. Fu, H. Lei, Y. Zhang, B. Ren, M. Zhong, J. Yang and J. Zheng, Integration of Antifouling and Antibacterial Properties in Salt-Responsive Hydrogels with Surface Regeneration Capacity, J. Mater. Chem. B, 2018, 6, 950–960.
- 37 B. D. Boer, H. K. Simon, M. P. L. Werts, E. W. v. d. Vegte and G. Hadziioannou, "Living" Free Radical Photopolymerization Initiated from Surface-Grafted Iniferter Monolayers, *Macromolecules*, 2000, **33**, 349–356.
- 38 M. Dan, S. Yang, X. Xin, S. Li and W. Zhang, A New Family of Thermo-Responsive Polymers Based on Poly[*N*-(4-vinylbenzyl)-*N*,*N*-dialkylamine], *Macromolecules*, 2013, **46**, 3137–3146.
- 39 H. X. Wu, L. Tan, Z. W. Tang, M. Y. Yang, J. Y. Xiao, C. J. Liu and R. X. Zhuo, Highly Efficient Antibacterial Surface Grafted with a Triclosan-decorated Poly(*N*-Hydroxyethylacrylamide) Brush, *ACS Appl. Mater. Interfaces*, 2015, 7, 7008–7015.
- 40 C. Zhao and J. Zheng, Synthesis and Characterization of Poly(*N*-hydroxyethylacrylamide) for Long-term Antifouling Ability, *Biomacromolecules*, 2011, **12**, 4071–4079.
- 41 C. Zhao, L. Li, Q. Wang, Q. Yu and J. Zheng, Effect of Film Thickness on the Antifouling Performance of Poly(hydroxyfunctional methacrylates) Grafted Surfaces, *Langmuir*, 2011, 27, 4906–4913.
- 42 J. Yang, M. Zhang, H. Chen, Y. Chang, Z. Chen and J. Zheng, Probing the Structural Dependence of Carbon Space Lengths of Poly(*N*-hydroxyalkyl acrylamide)-Based Brushes on Antifouling Performance, *Biomacromolecules*, 2014, **15**, 2982–2991.
- 43 M. Orhan, D. Kut and C. Gunesoglu, Improving the Antibacterial Activity of Cotton Fabrics Finished with Triclosan by the Use of 1,2,3,4-Butanetetracarboxylic Acid and Citric Acid, *J. Appl. Polym. Sci.*, 2009, **111**, 1344–1352.
- 44 W. Zhang, P. K. Chu, J. Ji, Y. Zhang, X. Liu, R. K. Fu, P. C. Ha and Q. Yan, Plasma Surface Modification of Poly Vinyl Chloride for Improvement of Antibacterial Properties, *Bio-materials*, 2006, 27, 44–51.
- 45 L. Huang, L. Zhang, S. Xiao, Y. Yang, F. Chen, P. Fan, Z. Zhao, M. Zhong and J. Yang, Bacteria killing and release of salt-responsive, regenerative, double-layered polyzwitterionic brushes, *Chem. Eng. J.*, 2018, 333, 1–10.
- 46 B. Wu, L. Zhang, L. Huang, S. Xiao, Y. Yang, M. Zhong and J. Yang, Salt-Induced Regenerative Surface for Bacteria Killing and Release, *Langmuir*, 2017, 33, 7160–7168.